EUROPEAN COMMISSION

nuclear science and technology

Fracture Mechanics Based Embrittlement Modelling (FRAME)

Authors
Matti Valo (1), Enrico Lucon (2), Milan Brumovsky (3)
Beatriz Acosta (4), Luigi Debarberis (4), Jyrki Kohopää (5)
Ferenc Gillemot (6), Marta Horwath (6), Ulla Ehrnstén (1)

(1) VTT, Finland
(2) SCK•CEN, Belgium
(3) UJV/REZ, Czech Republic
(4) JRC-IE, EC, the Netherlands
(5) Fortum Nuclear Services, Finland
(6) AEKI (KFKI), Hungary

Contract N^{o} FIKS-CT-2000-00101

Final report

Work performed as part of the European Atomic Energy Community's R&T specific programme
Nuclear Energy 1998-2002, key action Nuclear Fission Safety (Fifth Framework Programme)
Area: Operational safety of existing installations

Directorate-General for Research
2007 Euratom

The FRAME project shows that fracture toughness characterisation of irradiated materials using small three-point bend specimens can be made consistently and without bias between the partner laboratories according to the Master Curve standard ASTM E1921. Tight descriptions for the embrittlement shifts based on material chemistry were derived in the project. The shifts were described by copper, phosphorus and nickel terms. Pressure vessel steels and model alloys were studied in the project. Sensitivity of model alloys to phosphorus impurity content was found to be five times higher than sensitivity of steels as concerns transition temperature shifts. Model alloys also have large portions of intergranular fracture on specimen fracture surfaces, which is assumed to explain the difference in the behaviours.

FRAME data were also compared with several Charpy-V-based trend curves. The PNEA and Reg. Guide 1.99-rev.1 were observed to work well when applied to relevant types of materials. The shift formula derived from the FRAME data works better than any trend curve formulas and the explanation is believed to be in the single parameter irradiation behind the data. The FRAME database is small and the FRAME formula is not proposed to be used as a trend curve. However, FRAME data suggests that creation of more generic trend curves might be feasible if variation of material chemistry, neutron doses, and irradiation temperatures inherent in large surveillance databases could be minimised.

Preface

FRAME (Fracture Mechanics Based Embrittlement Modelling) was a Euratom FP5 shared-cost project realised by a consortium where VTT was acting as the coordinator and SCK•CEN, UJV/REZ, JRC-IE Petten, KFKI, and Fortum Nuclear Services as partners.

Espoo (Finland), May 2007

The authors

Contents

1 Introduction 1

2 Objectives of FRAME 1

3 Research programme 2

3.1 Choice of specimen size and geometry 2
3.2 Selection of materials 3
3.3 Specimen manufacture, prefatigue and side-grooving 5
3.4 Specimen irradiation 5

4 Experimental and analytical methods 6

4.1 Master Curve analyses 9
4.2 SINTAP analysis 9

5 The measured data 10

6 QA analyses of fracture toughness data 10

7 Modelling of chemistry factors 16

7.1 Derivation of chemistry factors 16

8 Summary of SEM studies of some specimen fracture surfaces 19

9 Comparison of FRAME data with Charpy-V-based trend curves 20

9.1 Regulatory Guide 1.99-Revision 1 20
9.2 PNAE formula for VVER 440 welds 21
9.3 Tentative FRAME descriptions 22

10 Summary 25

11 References 27

1 Introduction

Traditionally fracture properties in the irradiated material condition have been assessed by measuring fracture toughness (lower bound curve) in the unirradiated condition and by assuming that irradiation shift in the transition temperature can be estimated by the Charpy-V test [1]. Often the Charpy-V-based shift correlates well with the fracture toughness shift but this is not always the case [2]. The objective of FRAME was to promote the use of the direct-measurement elastic plastic fracture toughness parameter K_{JC} for the irradiated materials. K_{JC} is a physical measure for material resistance to fracture. It can be utilised directly in PTS analysis.

In the project the T_0 transition temperatures of 30 different materials were measured according to the Master Curve standard in the unirradiated as well as in the irradiated conditions. The specimens were irradiated in the HFR in Petten and in the Budapest Research Reactor and they were tested by VTT, SCK•CEN, UJV/REZ and KFKI. Altogether 736 fracture toughness specimens were tested in the project. Only one specimen capsule was irradiated in the HFR in Petten (containing the majority of specimens) and hence chemistry factor but not the fluence dependence of embrittlement could be derived from the created data. The derived embrittlement response of the materials was compared with some published Charpy-V test-based trend curves.

2 Objectives of FRAME

It is well known that the properties of pressure vessel materials, which are exposed to fast neutrons, may change considerably during the lifetime of the reactor. Hence the structural integrity analyses of the reactor vessel need to be updated from time to time due to material ageing. Pressurised thermal shock is the relevant accident concept. The analyses require fracture toughness of the structural materials, loads in the vessel wall and cracks in the structure as input parameters.

A sharp fatigue crack is the most severe type of defect and material resistance to loading of sharp cracks is described by fracture toughness. Practically always cleavage initiation properties are needed in the pressure vessel analyses. Cleavage fracture often occurs also in a Charpy-V test as one of the fracture processes and due to historical reasons the estimation of the effect of irradiation on material properties is based on the Charpy-V test. However, there are basic differences between the Charpy-V and the fracture toughness tests, i.e. notch versus sharp crack, dynamic versus static loading and initiation plus crack advance versus pure initiation. Hence direct measurement of initiation fracture toughness of the irradiated material is the ideal method to characterise ageing of materials.

Recent developments in elastic-plastic fracture toughness methodologies and especially the issue of the Master Curve standard, *ASTM E1921-97, Standard Test Method for Determination of Reference Temperature, T_o, for Ferritic Steels in the Transition Range*, allow direct determination of the cleavage initiation fracture toughness transition temperature T_0 with a relatively small number of small-size specimens. Hence direct fracture toughness tests can be used equally well as Charpy-V tests for vessel surveillance. Currently all formal descriptions of transition temperature shift as a function of neutron fluence, material impurity

content, and irradiation temperature are based on the Charpy-V test, because large databases are available only for Charpy-V tests. Overview of published trend curves is given in [3].

In addition to full relevance of the measured K_{JC}-values for structural analyses, the Master Curve offers also other superior features. Due to the constant shape of the curve, K_{JC} values can be measured within a narrow temperature range (or at single temperature), which is not the case with Charpy-V transition curves. This feature reduces the required amount of testing considerably and consequently also the costs. In addition, statistical scatter of initiation fracture toughness K_{JC} is well modelled and hence confidence limits for the measured data can be easily derived.

The objective of FRAME is to prove that the measurement of K_{JC} is a practical, consistent and laboratory-independent way of material characterisation. In FRAME a database is created, even if relatively small, which is compared to Charpy-V-based trend curves. In addition, the database is used to derive a model for embrittlement shifts as a function of chemical impurity contents of the materials. The single parameter irradiation is a good basis for modelling but it is clear that the number of data created in the project is far too small for giving a firm status for the created models.

3 Research programme

3.1 Choice of specimen size and geometry

It is clear that the number of different irradiated materials should be relatively high in order to reach the objectives of the project. For ease of specimen manufacture and for good packing density of specimens into the irradiation capsule the three point bend specimen geometry was chosen. Side grooves of 2 x 10 % were used for all specimens, because side grooving is supposed to increase specimen constraint and in addition it also improves the straightness of the pre-fatigue crack front in the specimen. The validity window of measured K_{JC}-values according to ASTM E1921 is schematically shown in Figure 1. It is clear that on the temperature scale the target specimen test temperature shall be near the T_0-50 ^oC side of the temperature range in order for cleavage fracture to occur in the test and the K_{JC} value to be below the validity limit of M = 30. The upper limit value of K given by (1) depends on yield strength and on specimen size. A specimen cross-sectional dimension of 5 mm(B) x 10 mm(W) was chosen to be used in the programme as it was considered a proper compromise between the number of materials, which can be packed into the irradiation capsule, and the specimen size dependent validity limit of K_{JC}. The specimen used in the project is shown in Figure 2.

$$K_{JC(\lim it)} = (Eb_o R_{p0.2\%} / 30)^{1/2} \qquad (1)$$

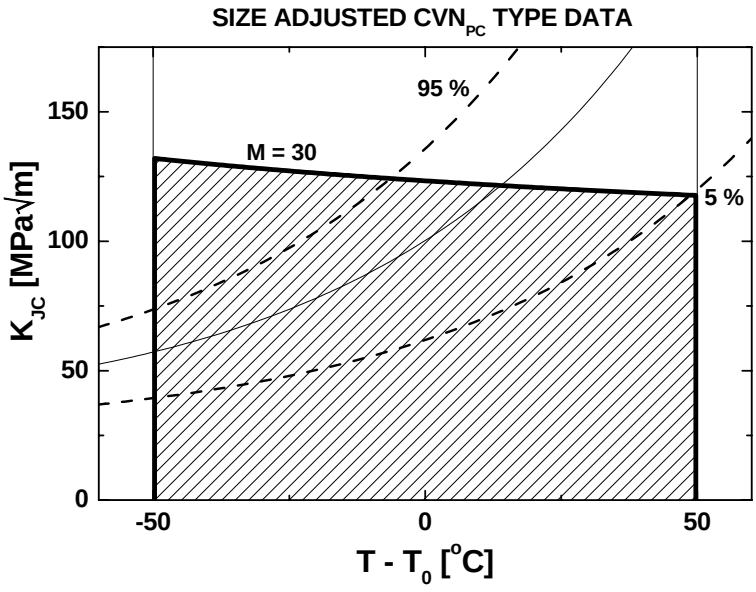

Figure 1. Test temperature versus K_{JC} window according to ASTM E 1921 for valid tests. The probability to get a valid data point is highest near the left-hand side of the temperature window

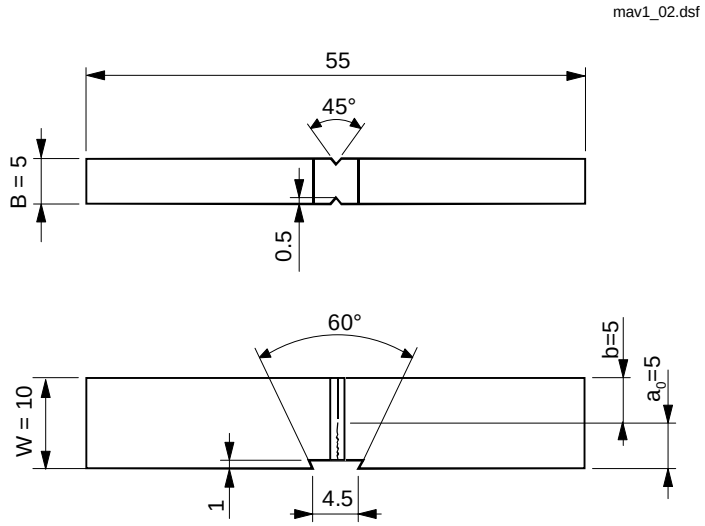

Figure 2. The nominal dimensions of the 3PB specimens. Integral clip seats were used only in the VTT tested specimens. Specimens, which were machined from broken halves of Charpy-V specimens, had B = 4.85 mm

3.2 Selection of materials

The aim was to include into the test matrix mostly steels (plate, forging and weld materials), which have relatively high impurity content in order to get well defined, relatively large embrittlement shifts. In practice the supply of steels was rather limited and the test matrix was complemented with model alloys. With this choice the distribution of materials in the copper-

phosphorus-nickel space could be covered relatively evenly but the value of the data in describing steel behaviour was reduced. Both Western and Russian type steels were selected. Distribution of copper, phosphorus and nickel contents in FRAME materials is shown in Figures 3-5. The FRAME materials are identified in Table 2 below.

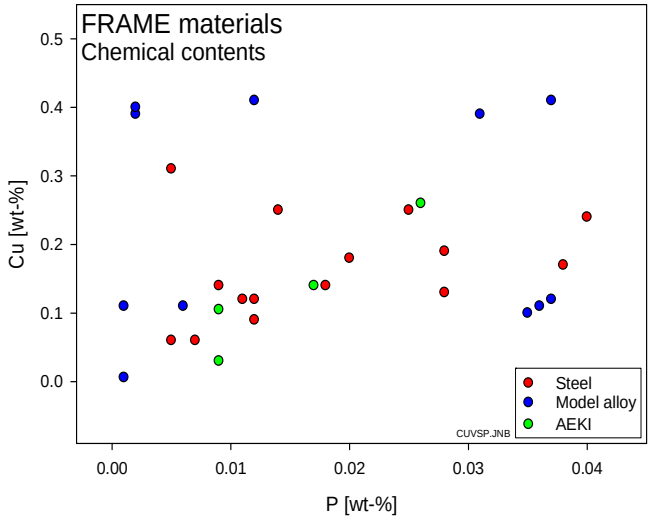

Figure 3. Copper and phosphorus contents of FRAME materials

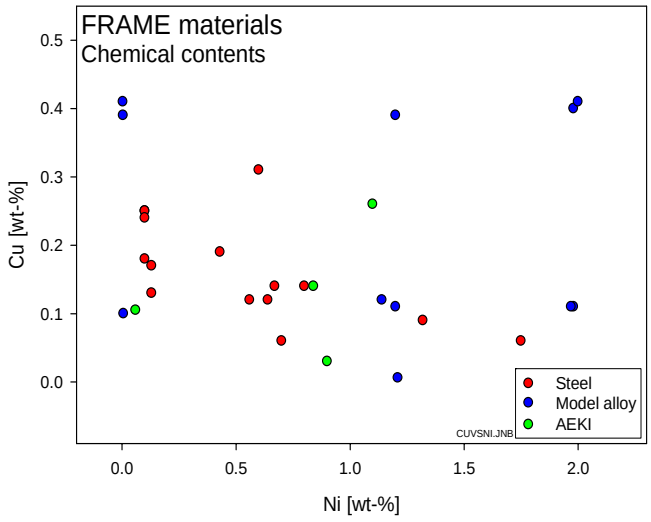

Figure 4. Copper and nickel contents of FRAME materials

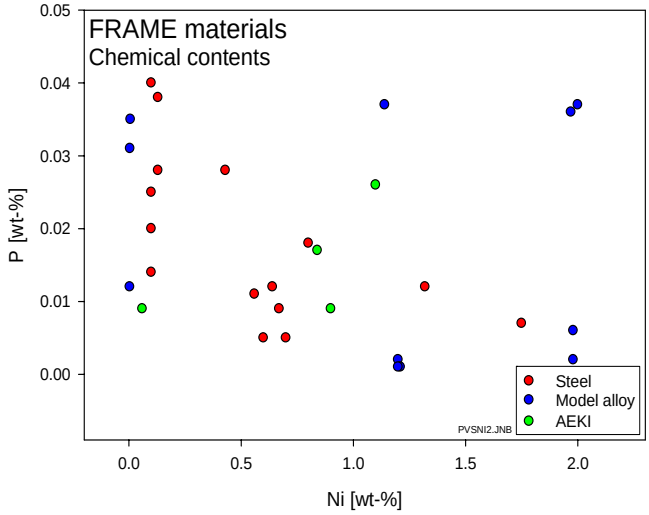

Figure 5. Nickel and phosphorus contents of FRAME materials

3.3 Specimen manufacture, prefatigue and side-grooving

All specimens were manufactured at one site. Both the unirradiated specimens and specimens to be irradiated were manufactured at the same time and specimen orientations and locations in both groups were kept the same and unbiased by random sampling. The specimens were pre-fatigued and side grooved at VTT as it was assumed that specimen preparation by one laboratory may reduce possible inhomogeneity in specimen finish.

In principle the specimens should be pre-fatigued in the irradiated condition. However, this would have lead either to cross-transport of specimens between the partners or possibly variation in the pre-fatigue and side-grooving procedures at different testing laboratories. As a compromise the standard specimens were pre-fatigued before irradiation with a low nominal final K_{max} of 10 MPa$\sqrt{}$m. Chemistry of all materials was analysed by VTT with the Optical Emission Spectrometer “Spectrolab S”.

3.4 Specimen irradiation

Specimen irradiation was performed by JRC-IE in the HFR in Petten and by AEKI in the Budapest Research Reactor. One Lyra irradiation capsule used in the HFR in Petten was allocated to the project. Hence embrittlement shifts could not be measured as a function of neutron fluence but instead the irradiation offered a good opportunity to compare embrittlement shifts of different materials in a single parameter irradiation and to derive chemistry factors. Two subsequent capsule irradiations were performed in the Budapest Research Reactor. The specimens, which were included in the initial FRAME programme and which were tested by NRI, SCK•CEN and VTT in the irradiated condition, were irradiated in HFR in Petten and the specimens studied by AEKI, were irradiated in the Budapest Research Reactor. Both irradiations are described below.

Pressure vessel steels from different vessel manufacturers were included in FRAME. The target irradiation temperature was defined to be 280 ^{o}C. This value is a compromise between

the assumed vessel wall temperature of 270 ^{o}C in VVER-440 units and 290 ^{o}C in many Western units and in the VVER-1000 units.

LYRA is an irradiation rig in the Pool Side Facility (PSF) of the HFR in Petten. A radiation shield plate of tungsten is installed between the reactor core and the sample holder and gamma heating in the location of the sample holder is < 0.15 W/g. The Lyra irradiation capsule with specimen/sample packing is shown in Figure 6.

Standard neutron dosimeters Fe, Co, Ti, Ni, Cu and Nb were utilised for dose determination in the irradiation capsules.

The FRAME irradiation was completed within 5.3 HFR reactor cycles (132.55 full power days) in Petten. Although the specimen holder was vertically rotated 180 degrees after about 3.45 HFR cycles of the irradiation campaign, the accumulated doses measured for the four vertical capsule corner lines showed substantial differences as can be seen in the Figure 7. It was noticed that the position of the capsule relative to reactor core during the first and second halves of irradiation in HFR in Petten was not equal. The derived specimen fluences and fluence rates are given in Table 1.

The target irradiation temperature was 280 ^{o}C. Temperature was controlled largely in the HFR Petten by the gas mixture located between the sample holder and the outer containment and the fine control was performed by active heaters. The central plate of the specimen holder was instrumented with 24 thermocouples. Temperature monitoring in both irradiation reactors indicates that temperature stability of the irradiation capsule was good.

Table 1. Neutron exposures in the AEKI irradiation in the Budapest Research Reactor (BRR) and in Lyra-04 irradiation in the HFR in Petten

Reactor	Material	Code	Irradiation time	Fluence 10^{19} n/cm^2, E > 1MeV	Fluence rate 10^{12}n/cm^{2}s, E > 1MeV
BRR	Gr-8 weld	g	234 h	5.0	60
BRR	JWP	p	234 h	4.2	50
BRR	JWQ	w	234 h	3.3	40
BRR	JRQ	j	234 h	3.05	36
HFR Petten	all other*	all other*	132.6 d	1.75-2.9	1.5-2.5

* 26 materials each with approximately 12 specimens.

4 Experimental and analytical methods

Tensile data ($R_{p0.2\%}$) are required in the analyses of fracture toughness data for determining the validity limit of the measured K_{JC} values. Tensile test specimens were not included into the irradiation capsules, because it would have reduced the number of materials to be irradiated. Instead small flat tensile specimens were prepared with EDM from the broken halves of tested 3PB specimens. Tensile data were created for all irradiated materials and for model alloys in the unirradiated condition. Tensile data for steels in the unirradiated condition was collected from literature or received from the material suppliers. Tensile tests were performed at room temperature only and the yield strength value at test temperature was estimated from the Welding Institute formula [4].

In fracture toughness testing each partner used his own standard testing technique and consistency of testing was checked by the QA-procedure reported in Chapter 6. Loading rate of 0.1 mm/min was agreed to be used in the tests. Each partner reported for each test the following parameters: test temperature, specimen dimensions, initial and final crack lengths, load and deflection values corresponding to cleavage initiation (or ductile end of test) and the J^C and K_{JC} values calculated according to ASTM E1921.

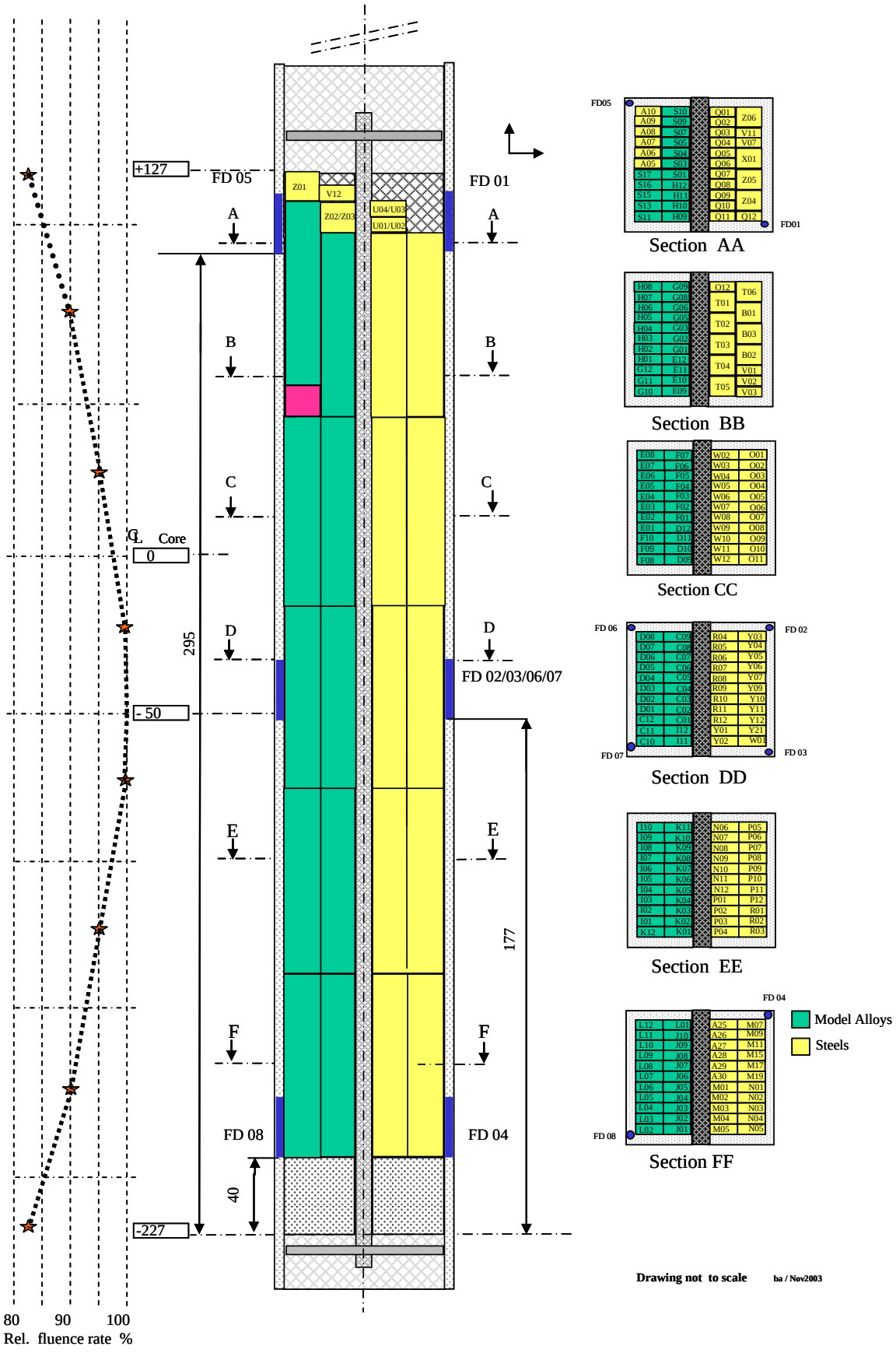

Figure 6. The loading of FRAME specimens into the LYRA irradiation capsule. Altogether 288 specimens equivalent to size 5 x 10 x 55 mm were loaded in the capsule

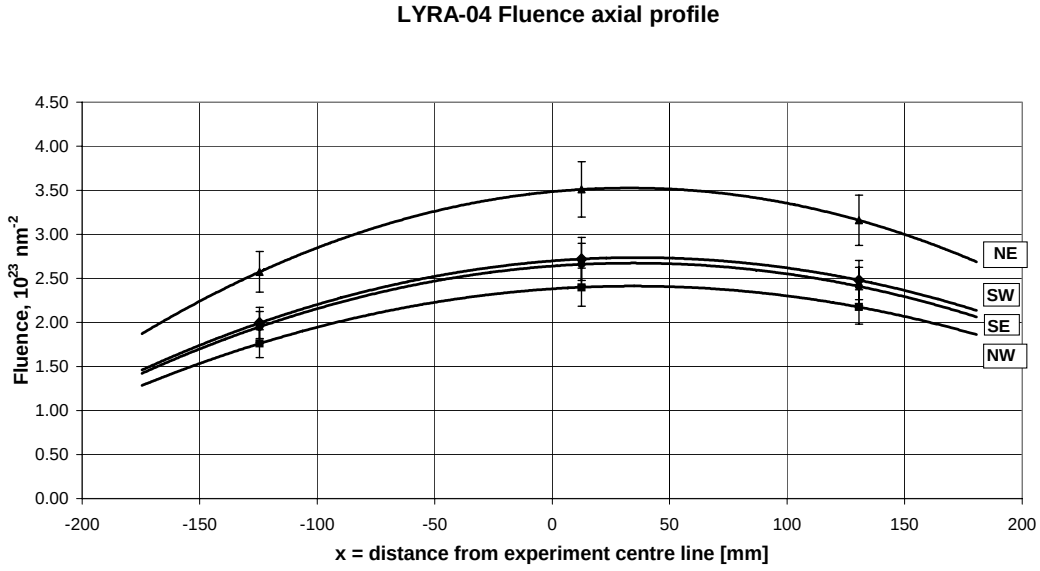

Figure 7. Vertical neutron fluence distribution along the four capsule corner lines NE, SW, SE and NW. The points with error bars identify the corner positions of the capsule (top, middle and bottom)

4.1 Master Curve analyses

The multitemperature approach and data censoring was applied in the Master Curve analyses of the data. In the cencoring procedure those K_{JC} values which are higher than the validity limit (1) are lowered to the validity limit and they are treated as ductile end-of-test values. The T_0 values are derived from the maximum likelihood estimation

$$\sum_{i=1}^{n} \frac{\delta_i \cdot \exp\{c \cdot [T_i - T_0]\}}{a - K_{min} + b \cdot \exp\{c \cdot [T_i - T_0]\}} - \sum_{i=1}^{n} \frac{(K_{Jc\,i} - K_{min})^4 \cdot \exp\{c \cdot [T_i - T_0]\}}{(a - K_{min} + b \cdot \exp\{c \cdot [T_i - T_0]\})^5} = 0 \quad (2)$$

where a = 31, b = 77 and c = 0.019. $\delta_i = 1$ when the measured value refers to valid cleavage initiation data point and $\delta_i = 0$, when the value is a valid end-of-test ductile value or a censored value lowered to the specimen size and yield strength dependent validity limit value (1).

4.2 SINTAP analysis

SINTAP analysis [5] was also applied to the data. The SINTAP procedure identifies a lower population T_0 value of bimodal data, i.e. of data, which are composed of two separate populations. This analysis can define a lower limit T_0 for inhomogeneous data. According to the SINTAP procedure the data, which lies over the median curve, is censored, i.e. the data are lowered to the median line and it is treated as ductile end-of-test data. If the data follows the Master Curve statistics, the same T_0 values will be derived from the standard fit and the SINTAP fit. The statistical weight of the SINTAP-fit is reduced as approximately only half of the cleavage initiation data is included in the fit and hence the derived Master Curve and SINTAP T_0 values may differ from each other due to different statistics.

5 The measured data

Sixty separate transition curves were measured in the project. Some examples are shown in Figure 8. A summary of yield strength and T_0 data is given in Table 2. The nominal specimen irradiation temperature in FRAME was 280 ^oC. If tests are performed at higher temperatures than the irradiation temperature, there is an evident risk of specimen annealing during the test. For three materials the specimen test temperatures are clearly higher than the irradiation temperature, i.e. specimens of model alloys 176, 182 and 185 in the irradiated condition were tested in the temperature range of 330-360 ^oC. For these materials the determined T_0 values shall be considered as lower limit estimates. Better experimental evaluation of T_0 values for these materials is not physically possible. As no studies on annealing behaviour of these materials were performed, the estimated T_0 values are used in the analyses without any correction.

The SINTAP fit revealed that model alloy 181 is clearly inhomogeneous as the SINTAP fit results in 80-90 ^oC higher transition temperatures both for the unirradiated as well as the irradiated material conditions.

6 QA analyses of fracture toughness data

Testing of standard size (5 ∗ 10 ∗ 55 mm) specimens, which were irradiated in the HFR in Petten, was divided equally between NRI, SCK•CEN and VTT in such a way that each laboratory tested four specimens of each batch of 12 specimens. This testing pattern allows analyses of data consistency between the laboratories to be made.

As a quality check the normalisation procedure [6] proposed by VTT is applied to the data. Normalised load and normalised J are plotted against normalised specimen deflection. Consistent data should fall on the same normalised curves. The normalised parameters are defined as

Normalised load $$\frac{F_c * W}{B * (W - a_f)^2 * R_{p0.2\%}} \quad (3)$$

Normalised J $$\frac{J_c}{W - a_f} \quad (4)$$

Normalised deflection $$\frac{\Delta_c}{W} \quad (5)$$

where

F_c	load at fracture
Δ_c	specimen deflection at fracture
J_c	J-value at fracture
a_f	crack length at fracture
$R_{p0.2\%}$	yield strength at test temperature
B, W	specimen thickness and width

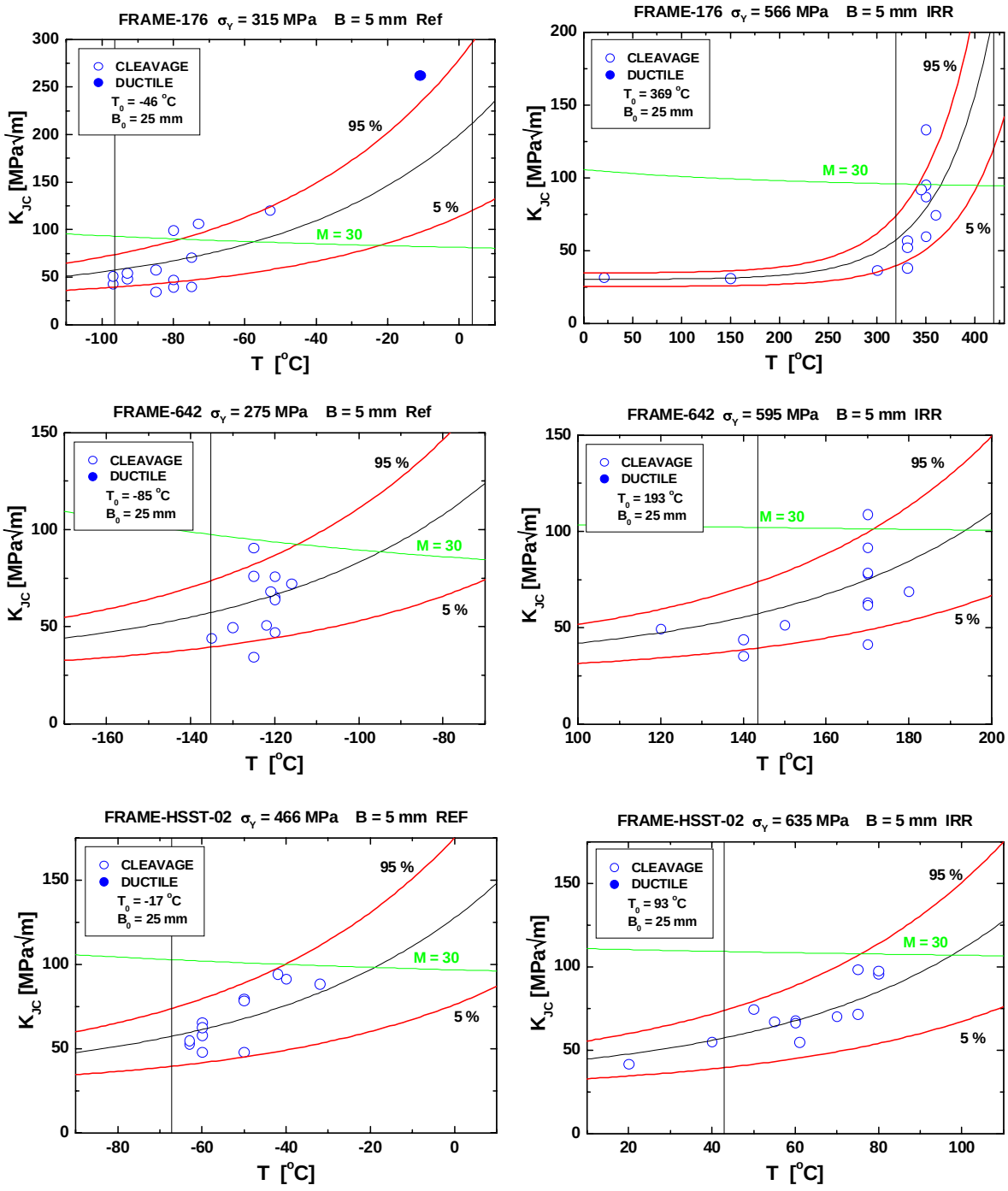

Figure 8. Transition curves (Master Curves) measured for model alloys 176 and 642 and steel HSST-02. The data for the unirradiated condition is on the left-hand side and the one for irradated condition on the right-hand side in the figure. Altogether 60 separate transition curves were created in the FRAME project

Table 2. Summary of chemistry, yield strength and Master Curve T_0 transition temperature data of FRAME materials

Material	Code	Cu	P	Ni	Dose	σ_y-ref	σ_y-irr	$\Delta\sigma_y$	T_0-ref	T_0-irr	ΔT_0
		%	%	%	*	MPa	MPa	MPa	°C	°C	°C
Model alloys											
176	C	0.120	0.037	1.14	2.69	315	566	251	-46	369	415
177	D	0.390	0.002	1.20	2.80	321	663	342	-72	275	347
181	E	0.110	0.006	1.98	2.91	277	547	270	-138	146	284
182	F	0.110	0.036	1.97	2.87	342	587	245	-125	359	484
183	G	0.400	0.002	1.98	2.84	333	691	358	-95	286	381
185	H	0.410	0.037	2.00	2.82	369	659	290	-80	465	545
443	I	0.006	0.001	1.21	2.45	316	549	233	-54	140	194
444	S	0.110	0.001	1.20	2.61	343	552	209	-95	185	280
638	J	0.100	0.035	0.007	1.82	273	418	145	-144	21	165
640	K	0.410	0.012	0.004	2.34	269	470	201	-162	-61	101
642	L	0.390	0.031	0.005	1.88	273	595	322	-85	193	278
				aver.	*2.55*						
Steels											
EDF-BX	T	0.25	0.014	0.10	2.74	422	646	224	-80	38	118
EDF-BW	X	0.25	0.025	0.10	2.57	579	740	161	-73	37	110
EDF-WD	U	0.24	0.040	0.10	2.40	376	609	233	-68	85	153
Lo2W	B	0.18	0.020	0.10	2.73	467	650	183	-34	70	104
JSPS	Z	0.19	0.028	0.43	2.35	461	643	182	2	124	122
FFA	Y	0.06	0.005	0.70	2.57	442	478	36	-110	-86	24
HSST02	P	0.14	0.009	0.67	2.25	466	636	170	-17	93	110
HSST03	Q	0.12	0.011	0.56	2.54	467	533	66	-25	52	77
HSST13	R	0.12	0.012	0.64	2.55	426	576	150	-104	-34	70
HSST73W	V	0.31	0.005	0.60	2.54	490	679	189	-103	45	148
JRQ	N	0.14	0.018	0.80	2.09	487	639	152	-72	50	122
W501	A	0.17	0.038	0.13	2.32	502	613	111	-6	105	111
W502	M	0.13	0.028	0.13	1.75	470	547	77	-41	42	83
VVER1000B	O	0.09	0.012	1.32	2.75	608	698	90	-95	-46	49
VVER1000W	W	0.06	0.007	1.75	2.77	569	704	135	-102	-9	93
				aver.	*2.45*						
AEKI data											
JRQ	j	0.14	0.017	0.84	3.05	510	600	90	-79	63	142
JWP	p	0.03	0.009	0.90	4.23	535	740	205	-120	-81	39
JWQ	w	0.26	0.026	1.10	3.20	536	740	204	-108	61	169
Gr-8 weld	g	0.105	0.009	0.06	4.95	500	560	60	-40	-4	36

All the required parameters are well defined but incorrect values may easily be reported for the final crack length. If crack arrest occurs in the specimen and the specimen is broken after the test at liquid nitrogen temperature, the crack arrest location may be interpreted erroneously as the crack length corresponding to cleavage initiation. Overestimates of a_f-values lead to outliers above the normalised curves both in the normalised load and normalised J values, the deviation in the normalised load value being clearly larger.

The normalised curves are shown separately for model alloys and steels in Figures 9-12. A minor bias between SCK•CEN and NRI data is noticed in Figures 10 and 12. The NRI,

SCK•CEN and VTT data are further compared based on the determined T_0 temperatures from single laboratory data. Single partner tested only 4 specimens out of the total 12 specimens and hence there is uncertainty in the T_0 values based on low statistics. The comparison is shown in Figure 13, where no bias can be seen between the three testing laboratories. The conclusion from the QA analyses is that NRI, SCK•CEN and VTT data can be considered equivalent, which is very important as large part of the project data were produced by these laboratories.

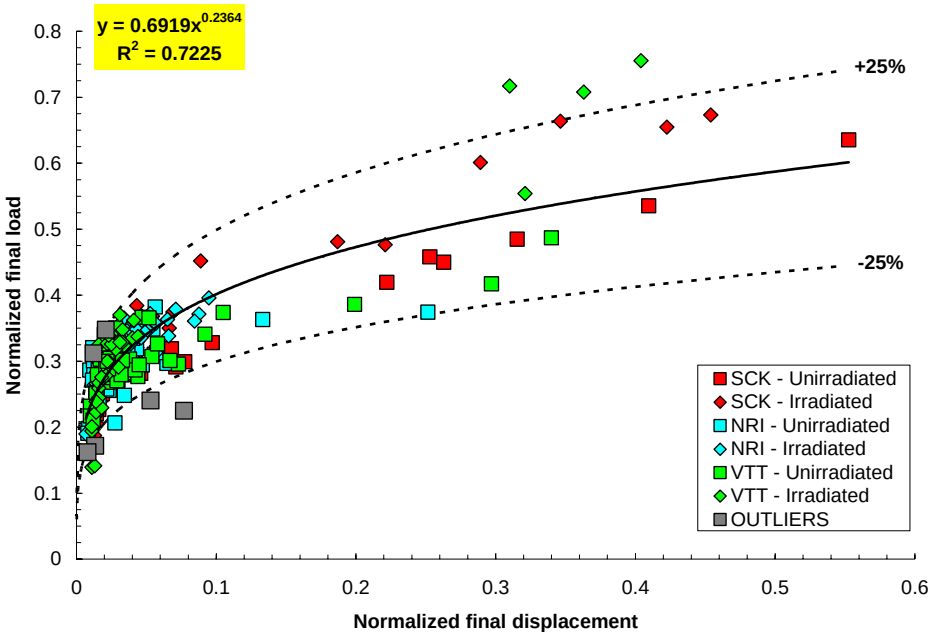

Figure 9. Model alloy data. Normalised end-of-test load versus normalised deflection. Both unirradiated and irradiated data are included. Outliers are data points falling outside the ± 25 % curves

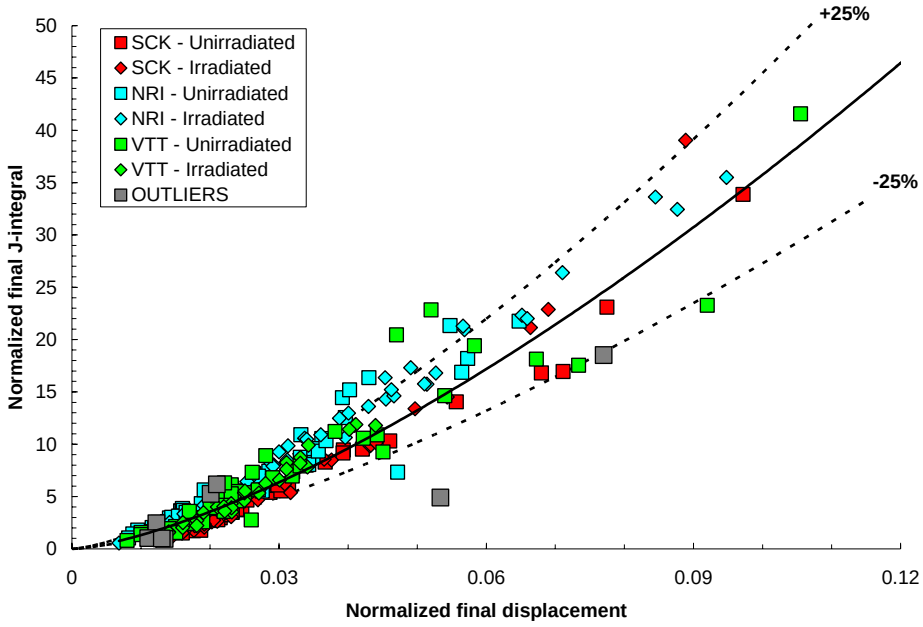

Figure 10. Model alloy data. The figure shows that SCK data lays slightly below the NRI data and VTT data roughly covers both data sets. Non-transparent points prevent the real distribution to be observed in the most populated areas

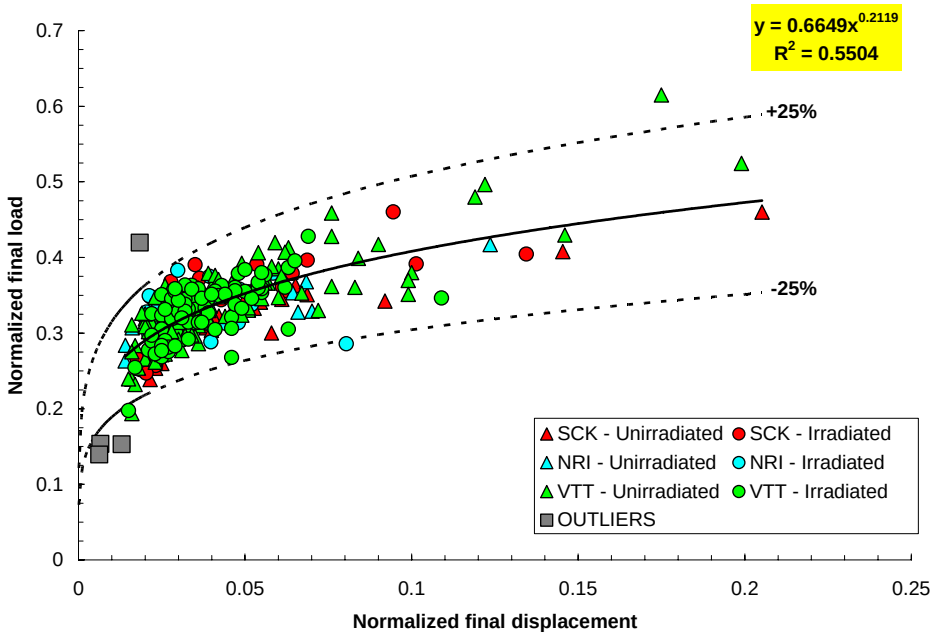

Figure 11. Steel data. Normalised end-of-test load versus normalised deflection. Both unirradiated and irradiated data are included

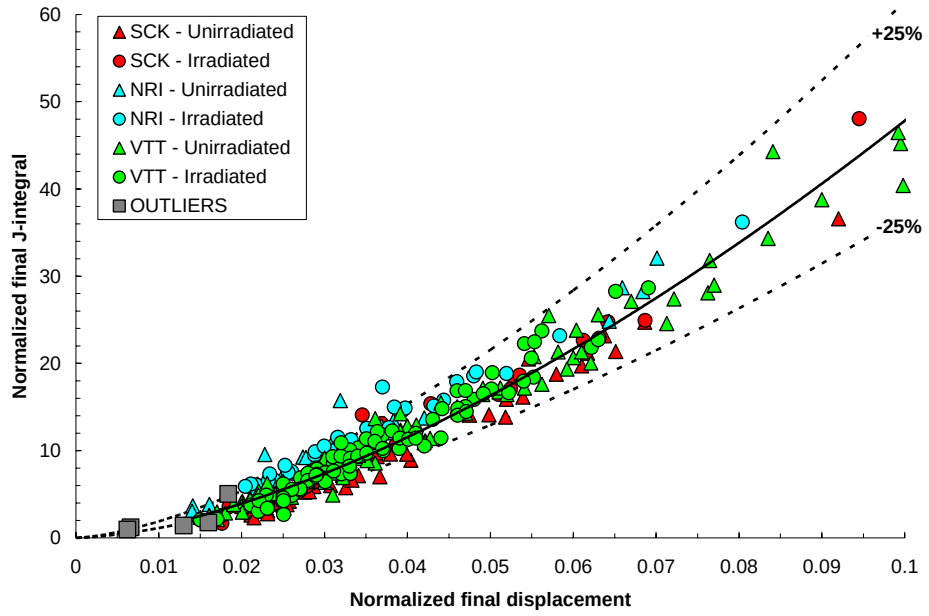

Figure 12. Steel data. Normalised end-of-test J versus normalised deflection. Both unirradiated and irradiated data are included. The figure shows that SCK•CEN data lie slightly below NRI data and that VTT data are located roughly between the two other data sets. However, non-transparent points prevent the real distribution to be observed in the most populated areas

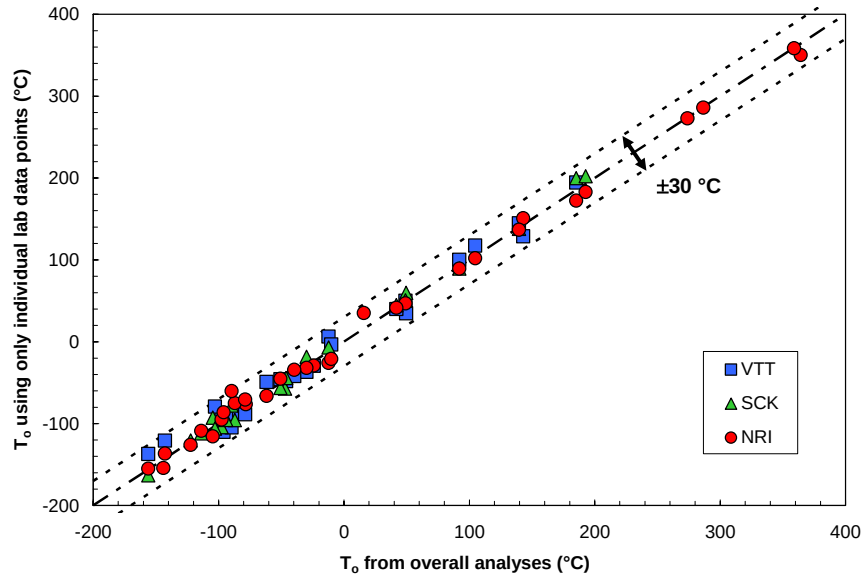

Figure 13. Comparison of the Master Curve transition temperature T_0 values based on NRI, SCK•CEN and VTT data. Data of model alloys and steels. T_0 based on the combined data (n = 12) is given on x axes and T_0 based on individual laboratory data (n = 4) is given on y axes. Statistical uncertainty in T_0 determination is approximately $\Delta T_0 = 18\ ^oC/\sqrt{n}$, i.e. $\Delta T_{0,x\text{-}axes} = 5\ ^oC$ and $\Delta T_{0,y\text{-}axes} = 9\ ^oC$. In reality the pure statistical uncertainty is larger because some data points give little or no contribution to the determined T_0 values, i.e. censored ductile end-of-test data and lower-shelf data

7 Modelling of chemistry factors

Transition temperature shift is traditionally described by a product of two terms, i.e. a chemistry factor term (CF) and a fluence term (FT)

$$\Delta T = CF(Cu, P, Ni) * FT(\text{fluence}, \text{fluence rate}) \quad (6)$$

The chemistry factor reflects the irradiation induced microstructural changes in the material but it is not straightforward to identify the microstructural formations or their composition from the derived chemistry factors. FRAME irradiation in the HFR in Petten was a single parameter irradiation as concerns irradiation temperature and neutron fluence, which should be a great advantice in modelling.

7.1 Derivation of chemistry factors

Homogeneity of neutron fluence within the JRC Lyra irradiation capsule was not prerfect and hence all measured irradiation shifts were normalised to the value of $2.5 * 10^{19}$ n/cm^2, E > 1 MeV according to the formula

$$\Delta T_{0,normalised} = \Delta T_{0,measured} * \left(\frac{2.50}{\Phi t} \right)^{1/3} \quad (7)$$

where Φt is the average neutron fluence of the specimens in each batch of irradiated materials. Normalisation is believed to improve the quality of the data even, if the applied exponent n = 1/3 may deviate from the real one (if any).

The number of possible trial functions for the chemistry factor is large but the search of the functions is started from simple ones. Single copper, phosphorus and nickel terms and pair multiplication terms are used. In addition an incubation term of phosphorus is included in the trial function having the general form

$$\Delta T = a_0 + a_1 * Cu + a_2 * (P - Po) * g(P - Po) + a_3 * Ni^{a4} + a_5 * P * Ni + a_6 * Cu * P + a_7 * Cu * Ni \quad (8)$$

where

$g(x) = 0$, if $x < 0$
$= 1$, if $x > 0$

Multiparameter regression fits were applied and the trials were started from simple descriptions and they proceeded into more complex ones. All the parameters in an acceptable fit shall be well defined, which in rough terms means that the absolute value of the parameter shall be higher than the uncertainty of the parameter. A good fit needs also to be balanced, i.e. the residuals of the fit must be randomly distributed in the parameter space. The identification of the best fits was rather unambiguous but there remains slight freedom in the final choise as concerns implications of slight improvements in the standard deviation (~ 0.2 ^{o}C). The best fit functions are identified as follows:

Model alloys

$$\Delta T = 281 * Cu + 6847 * (P - 0.012) * g(P - 0.012) + 195 * Ni^{0.39}\text{, SD = 33.2 }^{o}\text{C} \quad (9)$$

Steels

$$\Delta T_0 = 366 * Cu + 1366 * P + 39 * Ni\text{, SD = 17.2 }^{o}\text{C, without two high-nickel steels}$$
$$\Delta T_0 = 265 * Cu + 1860 * P + 348 * Cu * Ni\text{, SD = 20.6 }^{o}\text{C, all data} \quad (10)$$

The effect of nickel in steels is not ideally modelled as there are only two relatively high-nickel steels and in the rest of steels nickel is low and nearly constant. The fit without the two high-nickel points is clearly better than the fit with these steels. In addition, the Cu∗Ni term may be an artefact, which reflectes only the copper effect + low statistics.

The number of freedom, i.e. the number of data points minus the number of derived parameters, is in the model alloy fit 6 and in the lower standard deviation steel fit 10. The fits are shown in Figures 14-16.

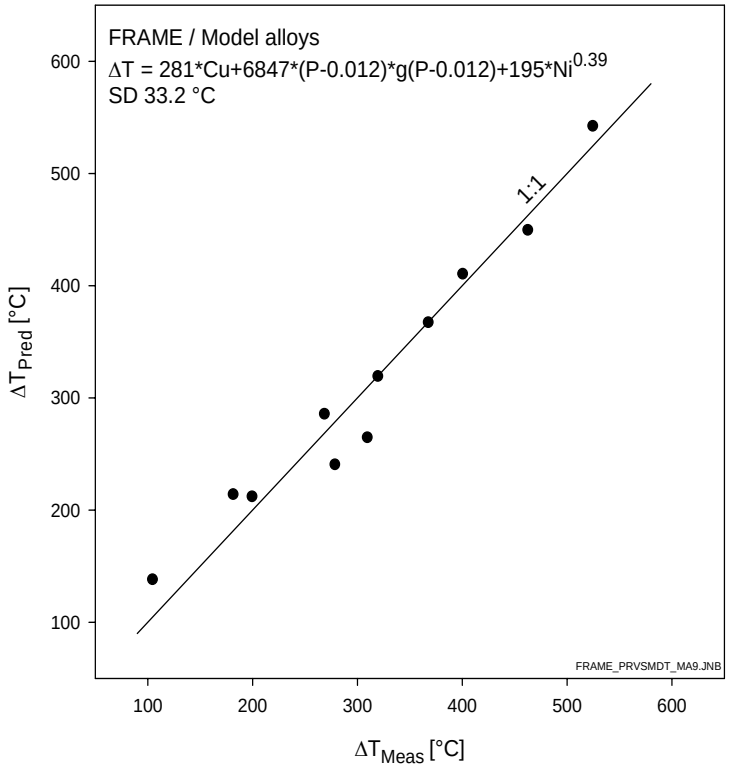

Figure 14. The best-fit description chemistry factor for model alloys

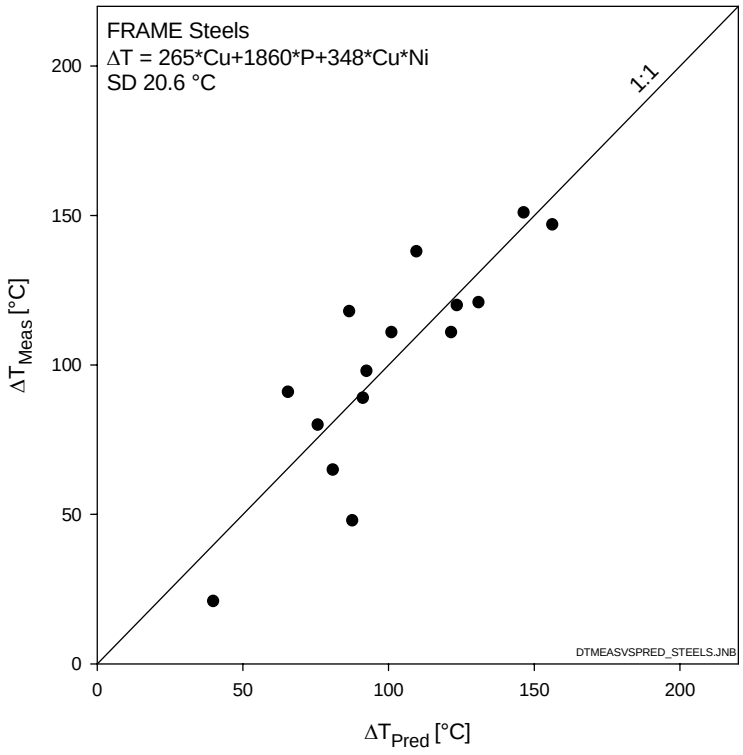

Figure 15. The best fit to steel data including the two high-nickel steels

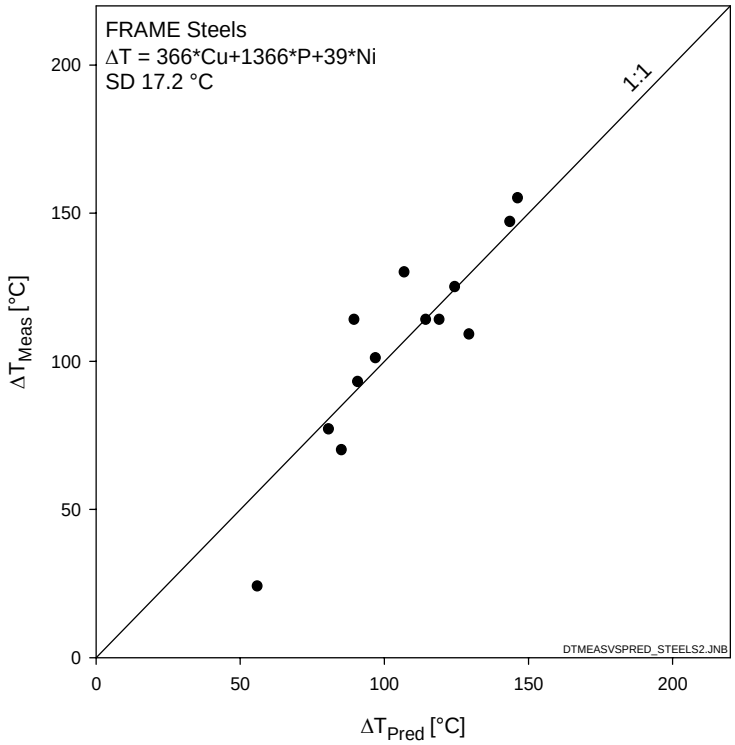

Figure 16. The best fit to steel data excluding the two high-nickel steels. The deviating low-shift point is FFA with Cu = 0.06 %, P = 0.005 % and N = 0.70 %, i.e. the general formula based on all data can not describe the nickel effect with absence of Cu and P

One noticeable feature in the good descriptions is that they have single element terms only. In the test matrix of model alloys as well as steels the key elements, i.e. Cu, P and Ni, vary widely and independently. If it is assumed that the key elements combine with certain rules (fixed proportions, threshold values, saturation contents etc.), wide and even coverage of the element space will average much of the details away. However, the best fits are supprisingly thight and hence the introduction of more complicated trial functions can not improve the fits considerable. Most of the model alloys showed large amounts of intergranular fracture in front of the crack tip as is later described. This is shown in the chemistry factor as enhanced phosphorus term. In spite of the occurance of intergranular fracture transition temperature shift for model alloys can be well described by material chemistry.

The relative contributions of the different chemistry factor terms depend on material chemistry. If an approximately average chemistry of steels of Cu = 0.15 %, P = 0.02 % and Ni = 0.5 % is chosen, the relative contributions to the predicted steel shift are: copper term 40 ^{o}C, phosphorus term 37 ^{o}C and CuNi term 26 ^{o}C. Hence no term in the chemistry factor of steels is a dominating one.

8 Summary of SEM studies of some specimen fracture surfaces

VTT characterised fracture surfaces of some model alloys and steels in the irradiated condition with SEM. The fracture modes have been identified and the proportions of different types of fracture surfaces, i.e. ductile, cleavage and intergranular type surfaces, were approximately quantified from the photographs. The characterisation was focused on the fracture surfaces ahead of the crack tip but photos were taken with varying magnifications covering the area from whole specimen halves down into sub-crystal sizes. Eight different model alloys were studied and the proportion of intergranular fracture ahead of crcak tip varied in these alloys betwwn 80-100 %, i.e. the fracture mode had been turned to intergranular almost completely. In steels no intergranular fracture was observed except in steels W501, where the proportion was 10 %. In spite of large IG portions the critical fracture in model alloys was clear and the load drop was large and sudded. A typical model alloy fracture surface is shown in Figure 17.

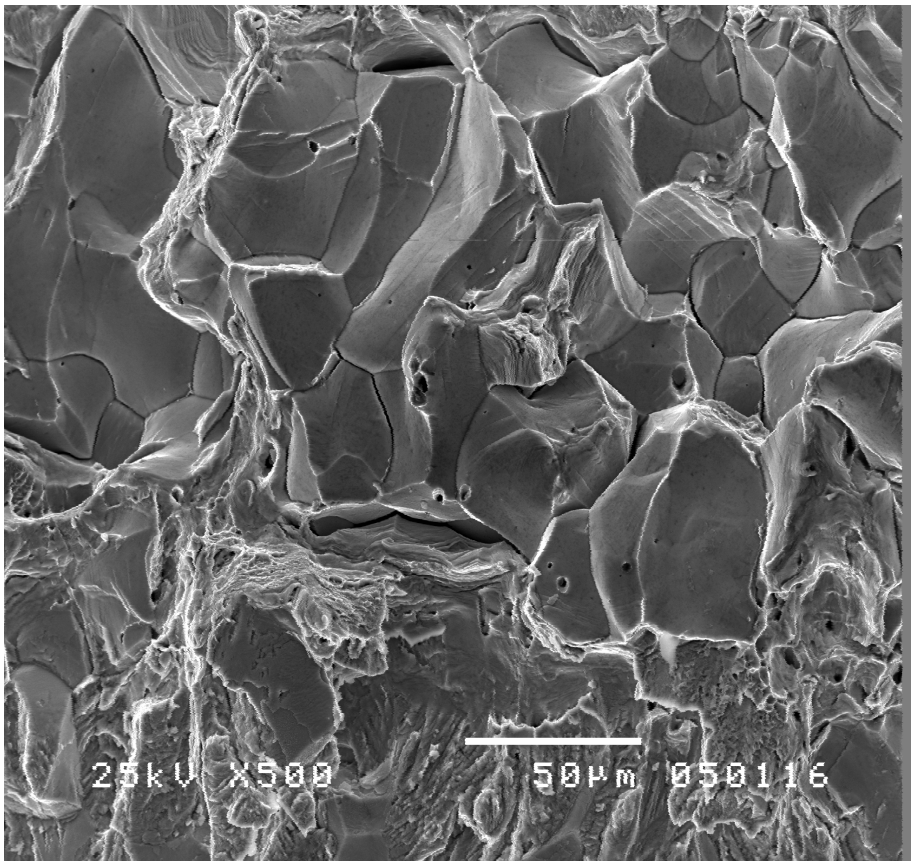

← Prefatigue crack tip

Figure 17. Model alloy 176, specimen C03, IG = 95 %, ductile 5 %, T = 331 ^{o}C, K_{JC} = 75MPa√m

9 Comparison of FRAME data with Charpy-V-based trend curves

Large number of Charpy-V-based trend curves has been published and copper, nickel and phosphorus contents are generally used for describing the chemistry factors. A collection of trend curves is given in reference [3]. Only comparisons with the US Regulatory Guide 1.99 Rev.1 and the PNEA for VVER 440 weld are shown as a figure in this report but more comparisons are given in Table 3. The comparison is made by plotting the prediction of the Charpy-V-based trend curve against the fracture toughness shifts measured in FRAME. The measured shifts and the average fluence values of each batch are directly used in the comparison, not the normalised shifts.

9.1 Regulatory Guide 1.99-Revision 1

This description dates back to 1977 and has the form (in degrees centigrade):

$$\Delta T_{CH-V} = \frac{5}{9} * \left[40 + 5000 * g(P - 0.008) * (P - 0.008) + 1000 * g(Cu - 0.08) * (Cu - 0.08)\right] * \Phi^{0.5}$$

where

$$g(x) \quad = 0, \text{ if } x < 0 \quad = 1, \text{ if } x > 0 \qquad (11)$$

The above function does not include nickel and hence it is not applicable to materials with high-nickel content. The comparison with the FRAME data is given in Figure 18. For steels the description is mostly conservative. The model alloy data are poorly described by this model.

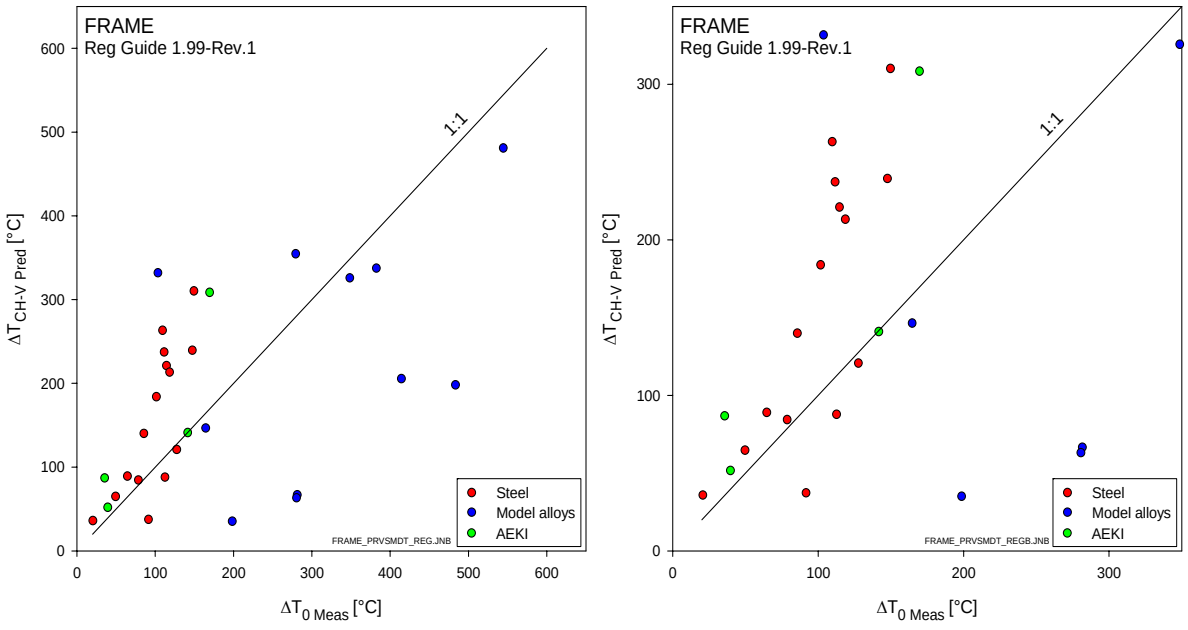

Figure 18. Comparison of FRAME data with the description of Regulatory Guide 1.99-Rev. 1. The right-hand side figure has magnified scales. AEKI = KFKI

9.2 PNAE formula for VVER 440 welds

PNAE is the Russian norm derived for VVER 440 weld metal. It has the form

$$\Delta T_{CH-V} = 800 * (P + 0.07 * Cu) * \left[\frac{\Phi t}{10^{18} n/cm^2, E > 0.5 MeV} \right]^{1/3} \qquad (12)$$

The PNAE norm uses neutron fluence in units of [10^{18} n/cm^2, E > 0.5 MeV]. Estimate for the fluence ratio in the Lyra capsule location in HFR in Petten is [E > 0.5 MeV] / [E > 1 MeV] = 1.7 (personal communication from Beatriz Acosta). In the Budapest Research Reactor the spectrum ratio is 1.4 as communicated by AEKI. The comparison of data with PNAE is shown in Figure 19. The formula does not include nickel and hence it should not be used for high-nickel steels.

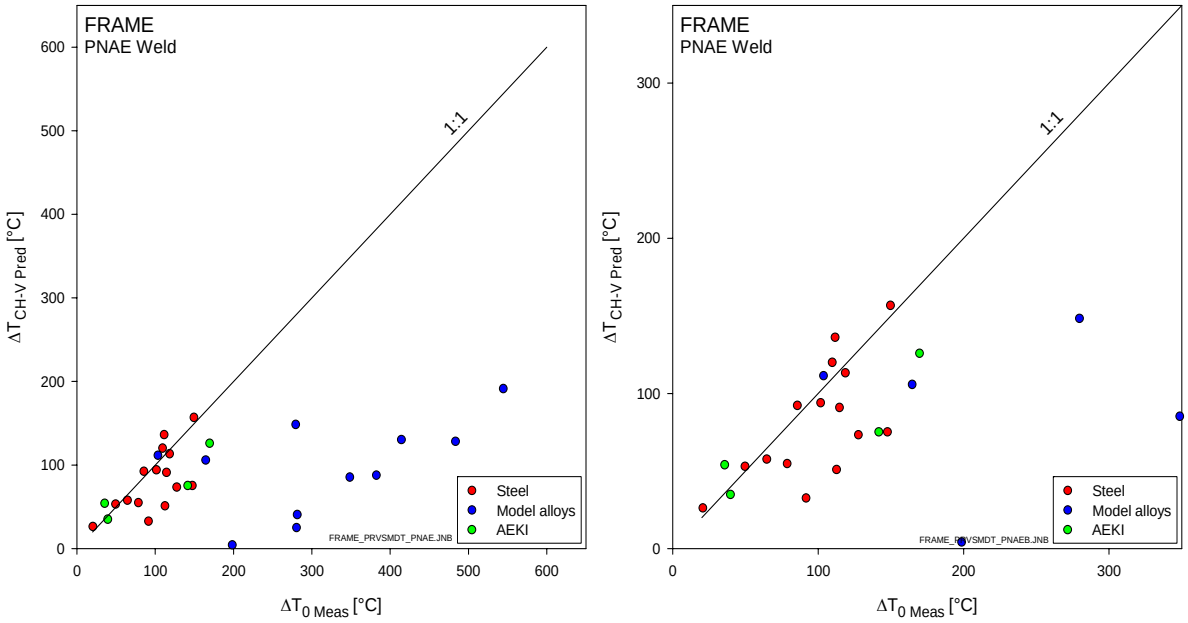

Figure 19. Comparison of FRAME data with the Russian PNAE formula. The norm is developed for VVER440 welds. AEKI = KFKI

9.3 Tentative FRAME descriptions

The tentative embrittlement descriptions derived in chapter 7 from FRAME data are also compared to the measured data in the similar manner as the Charpy-V-based trend curves. This is a comparison between the measured and predicted T_0 shifts, i.e. it shows the descriptive capability of the model. No Charpy-V tests were made in FRAME. The fluence dependence of n = 1/3 was used in data normalisation due to variation in the batch fluences. Neutron fluences and fluence rates in AEKI irradiation deviate considerably from the fluences in JRC-IE HFR irradiation.

Description of model alloys

$$\Delta T_0 = \left(281 * Cu + 6847 * (P - 0{,}012) * g(P - 0{,}012) + 195 * Ni^{0.39}\right) * \left(\frac{\Phi t}{2{,}5}\right)^{1/3}, \qquad (13)$$

SD = 33.2 °C

Description of steels

$$\Delta T_0 = \left(265 * Cu + 1860 * P + 348 * Cu * Ni\right) * \left(\frac{\Phi t}{2{,}5}\right)^{1/3}, \qquad (14)$$

SD = 20.6 °C

The data comparison is shown in Figure 20. Description (14) includes all steel data points. The steel description without the two high-nickel points shown in Figure 16 is clearly better (SD = 17.2 °C) than (14).

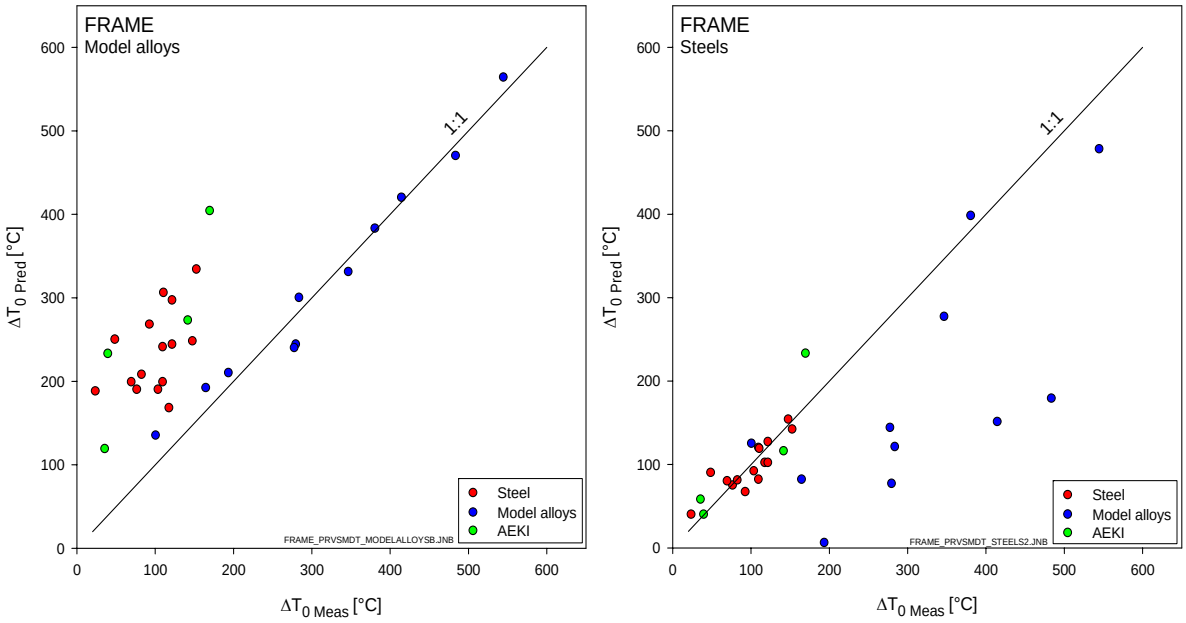

Figure 20. FRAME data versus FRAME model alloy prediction on the left-hand side and FRAME data versus FRAME steels prediction on the right-hand side

The steels have been grouped according to the steel/reactor type in Table 4, which allows a more detailed and correct comparison of the FRAME data with the trend curve predictions. The conclusion is that Reg. Guide 1.99-Rev.1 predicts the steel shifts in a conservative way except the slight over-prediction for HSST-02. The French FIM formula contains Cu, Ni and P contents as input parameters. It underpredicts the shifts for HSST-02, HSST-03 and JRQ. The Japanese JEPE formula includes Cu, P and Ni contents as well and it has clear tendency to under-predict the steel shifts as most of the shift ratios fall into the range of 1.1-1.7. The Russian formula PNAE, which does not include a nickel term, predicts quite well the shifts of VVER-440 welds. The Eason, Wrigth and Odette 1998 formula (EWO) is over-conservative for all steels.

The trend curve formulas describe the model alloy shifts poorly, as the descriptions have very large scatter and some of them show large discrepancies. Reg. Guide 1.99 Rev. 1 and the Eason, Wrigth, and Odette 1998 formulas give rough mean description for the model alloys but FIM, JEPE and PNAE largely underestimate the measured shifts. The general conclusion is that embrittlement proceeds much faster in model alloys than in steels. The apparent reason is qualitatively the much simpler structure of the alloys as compared to steels, i.e. irradiation enhanced diffusion proceeds much faster in model alloys than in steels due to lack of carbides and other sinks for vacancies and interstitial atoms, which mediate the structural changes under irradiation. As is described in chapter 8, most of the model alloys show large amount of intergranular fracture contrary to the steels, where intergranular fracture can be seen only exceptionally and in small proportions. Hence model alloys are inappropriate materials to be used for modelling steel embrittlement. Little work has been done in modelling cleavage/critical fracture in materials, which show large amount of intergranular fracture. The fact that model alloy embrittlement can be well described by the material chemistry, indicates that initiation of critical fracture is well and in detail controlled by microstructural features produced by irradiation.

Table 3. Comparison of measured and predicted steel shifts sorted according to steel types. PNAE formula is derived for VVER-440 welds and these materials in FRAME data are well described by this formula. Reg. Guide1.99-Rev. 1 has been derived for A533B materials and it describes these materials rather well. FIM and JEPE descriptions are also based on A533B data, but the descriptions do not work so well

Material	Code	Cu	P	Ni	Dose	ΔT_0 meas	ΔT_0, measured / ΔT, predicted					
							REG	FIM	JEPE	PNAE	EWO	FRAME
		%	%	%		^oC	-	-	-	-	-	Steel
VVER440 weld												
EDF-WD	U	0.24	0.040	0.10	2.40	150	0.5	1.1	1.2	**1.0**	0.3	**1.1**
Lo2W	B	0.18	0.020	0.10	2.73	102	0.6	1.2	1.4	**1.1**	0.4	**1.1**
W501	A	0.17	0.038	0.13	2.32	112	0.5	1.0	1.1	**0.8**	0.3	**0.9**
W502	M	0.13	0.028	0.13	1.75	86	0.6	1.2	1.3	**0.9**	0.3	**1.0**
Greif-8 weld	g	0.105	0.009	0.06	4.95	36	0.4	0.8	1.0	**0.7**	0.2	**0.6**
VVER440 base												
EDF –BX	T	0.25	0.014	0.10	2.74	115	0.5	1.2	1.3	1.3	0.5	**1.2**
EDF –BW	X	0.25	0.025	0.10	2.57	110	0.4	0.9	1.1	0.9	0.3	**0.9**
A533B												
HSST02	P	0.14	0.009	0.67	2.25	113	**1.3**	**1.9**	**1.9**	2.2	0.5	**1.3**
HSST03	Q	0.12	0.011	0.56	2.54	79	**0.9**	**1.5**	**1.4**	1.5	0.3	**1.0**
HSST13	R	0.12	0.012	0.64	2.55	65	**0.7**	**1.1**	**1.1**	1.1	0.3	**0.9**
HSST73W	V	0.31	0.005	0.60	2.54	148	**0.6**	**1.2**	**1.3**	2.0	0.6	**1.0**
FFA	Y	0.06	0.005	0.70	2.57	21	**0.6**	**0.6**	**0.9**	0.8	0.1	**0.6**
JRQ	N	0.14	0.018	0.80	2.09	128	**1.1**	**1.5**	**1.7**	1.8	0.4	**1.2**
JRQ	j	0.14	0.017	0.84	3.05	142	**1.0**	**1.5**	**1.7**	2.0	0.5	**1.2**
Model steels												
JSPS	Z	0.19	0.028	0.43	2.35	119	0.6	1.1	1.2	1.1	0.3	**1.0**
JWP	p	0.03	0.009	0.90	4.23	40	0.8	0.8	1.9	1.2	0.2	**1.0**
JWQ	w	0.26	0.026	1.10	3.20	170	0.6	0.8	1.1	1.4	0.4	**0.7**
VVER1000 high-nickel												
VVER1000B	O	0.09	0.012	1.32	2.75	50	0.8	0.6	0.9	0.9	0.2	**0.5**
VVER1000W	W	0.06	0.007	1.75	2.77	92	2.5	1.0	2.3	2.9	0.5	**1.4**

The FRAME based formulas give the best descriptions for model alloys as well as steels. FRAME descriptions are based on FRAME data only, i.e. on a limited database, and they have not been checked by other databases. Because fluence dependence of embrittlement could not be derived in FRAME, proper application of FRAME formulas to other databases is not directly possible. However, the fact that the number of derived parameters in FRAME formulas is much less than the number of data points, i.e. proper degree of freedom remains in the descriptions, and the wide variation of material chemistry of FRAME materials suggest that more accurate trend curve formulas can be derived, if only data in controlled single parameter irradiations with well defined materials could be created.

10 Summary

In the FRAME project, the effect of irradiation on 30 different materials was measured using the Master Curve transition temperature T_0 as a measure of toughness. Composition of all HFR irradiated materials was measured by one partner. The specimens were irradiated either in the JRC-IE HFR in Petten or in the Budapest Research Reactor. Most of the specimens were irradiated in the HFR in Petten in one irradiation capsule and this irradiation was in principle a single-parameter irradiation, i.e. irradiation temperature and neutron dose were the same for all specimens. However, even if the HFR capsule was rotated 180^o in the middle of the irradiation, fluence rates during the first and the second halves of the irradiation differed, which created additional inhomogeneity in the specimen fluences.

Integrity of the pressure vessel is the main concern in embrittlement studies and hence predominantly steels were studied in the project. Altogether 19 different steels including forgings and plates of A533B, VVER-440 and VVER-1000 type pressure vessel steels as well as weld metals were irradiated in the project. However, the acquisition of a good collection of steels with a wide variation of impurity contents was not possible within the allocated time and hence also 11 different model alloys were included in the programme. It turned out that the accumulated neutron fluence of $2.5 * 10^{19}$ n/cm^2, E > 1MeV in the HFR irradiation was enough to turn the model alloys into a predominantly intergranular fracture mode and hence the created model alloy data can not be used as support for modelling of steel behaviour.

One objective of FRAME was to promote direct fracture toughness characterisation of the irradiated material condition, whose data can be directly applied in integrity analyses of ageing pressure vessels. The Master Curve standard ASTM E1921 gives guidance on the measurement as well as application of the data. The data are in many respects superior to the current ASME procedure, which relies on the Charpy-V versus fracture toughness correlation (1:1 in shift). Testing of each batch of the HFR irradiated specimens was divided equally between the three testing laboratories, i.e. NRI, SCK•CEN and VTT. This division enabled to compare the data created in three different laboratories and the comparison described in Chapter 6 indicates that there is no observed bias in the determined T_0 temperatures between these laboratories.

The Master Curve standard has acceptance criteria for the measured K_{JC} values as concerns test temperatures (validity window of test temperatures in relation to T_0), the maximum measured K_{JC} values (to avoid general yielding) and the number of valid tests to guarantee statistically reliable estimates. The key point in testing is proper choice of test temperatures and homogeneity of the material. The used specimens were relatively small, i.e. B = 5 mm and W = 10 mm, and the model alloys in the unirradiated condition were relatively soft ($R_{p0.2\%}$: 270-370 MPa). This leads to a relative tight test window (in T versus K_{JC} plane) and some data were measured outside the approved range. However, meaningful T_0 values could be defined for all batches with the available 12 specimens. Some materials have slightly higher scatter than the Master Curve predicts, which is evidently an indication of material inhomogeneity.

Irradiation temperature of the specimens was 280 ^{o}C and irradiation damage starts to anneal when this temperature is clearly exceeded. Hence data of tests which have been performed at higher than the specimen irradiation temperature may be biased towards too low-measured transition temperatures. T_0 can not be derived from lower shelf tests and hence specimens of model alloys 176, 182, 185 in the irradiated condition had to be tested at temperatures 320-

380 ^{o}C, i.e. clearly over the irradiation temperature. The as-measured data were used in the analyses, because no information was available on the annealing behaviour of these materials. The measured shift of alloy 185 (highest test temperatures) was 545 ^{o}C and a moderate under-estimate of this value does not have much effect on the overall conclusions.

The measured T_0-based shifts could be described well with copper, phosphorus and nickel contents of the materials. The best description for model alloys is:

$$\Delta T_0 = \left(281 * Cu + 6847 * (P - 0{,}012) * g(P - 0{,}012) + 195 * Ni^{0.39}\right), \qquad \text{SD} = 33.2\ ^{o}\text{C}$$

The description is surprisingly good because the average shift measured with model alloys is approximately 350 ^{o}C. The estimated proportion of grain boundary fracture on specimen fracture surfaces ahead of the crack tip varies in the range of 80-100 %, which is a very high number and fully outside steel behaviour. Still the derived description is tight, which means that initiation of critical fracture is controlled in detail by the chemistry of the alloys. In general the model alloy specimens show a well-defined critical, unstable fracture. The percentage of IG-fracture can not be added as a parameter into the shift description because the percentage numbers are practically saturated. Five parameters are used to describe the data of the eleven model alloys, which means that six free parameters are described by the fit.

The best description for steel shifts, without the two high-nickel materials, is as follows

$$\Delta T_0 = \left(366 * Cu + 1366 * P + 39 * Ni\right), \qquad \text{SD } 17.2\ ^{o}\text{C}$$

This description is also reasonably good as the average measured shift is approximately 100 ^{o}C. FFA steel (Cu = 0.06 %, P = 0.005 %, Ni = 0.70 %) is the only material which clearly deviates from the fit, i.e. the formula does not describe well the effect of pure nickel, when Cu and P are missing. The average description may assume combination of nickel with copper or phosphorus and this combination is not possible in the FFA material. This steel description uses three parameters for describing thirteen data points.

The main difference between the model alloy and steel descriptions is the five times higher coefficient of the phosphorus term in the model alloy description as compared with the steel description. Model alloys have high, almost saturated portions of intergranular fracture on specimen fracture surfaces and the alloys do not contain carbon.

The FRAME data were also compared with some published Charpy-V-based trend curves. The trend curves should be applied within their range of application, which is not always clearly expressed in the literature. The Russian norm PNAE describes rather well the measured VVER-440 data and the Reg. Guide 1.99 Rev. 1 describes well the measured A533B data. The FIM and JEPE formulas are based on A533B-type steel data but the descriptions are less satisfactory. The Eason, Wrigth, and Odette formula from 1998 gives a poor description for the measured steel behaviour. The FRAME formula for steels works very well for all steels, which means that the current trend curves can be improved and generalised to materials which cover a wide variety of steels. The FRAME trend curve is based on FRAME data and this is the reason for its good applicability. However, there are only three fixed parameters, which are used for describing thirteen material data points of materials having wide variation of chemistry, i.e. the formula has a real description capability. The FRAME database is a limited one and the derived descriptions are not proposed to be used as

trend curves. The FRAME project, however, suggests that a single-parameter irradiation of a large number of different materials is required to derive a generic trend curve for steels.

11 References

[1] ASME Code Section III, Division 1 – NB-2331 (1995).

[2] Sokolov and R.K. Nanstad, *Comparison of Irradiation-Induced Shifts of K_{Jc} and Charpy Impact Toughness for Reactor Pressure Vessel Steels*, NUREG/CR-6609, November 2000.

[3] Petrequin, *A Review of Formulas for Predicting Irradiation Embrittlement of Reactor Vessel Materials*, EUR 16455 EN, AMES Report No.6, November 1996.

[4] British Standard BS7910:1999, *Guide on Methods for Assessing the Acceptability of Flaws in Fusion Welded Structures*, 8 April 1999.

[5] S.I.N.T.A.P., Structural Integrity Assessment Procedures for European Industry, Procedure – Final Version: November 1999, Chapter II.1.5.

[6] K. Wallin, *Master Curve Analysis of Ductile to Brittle Transition Region Fracture Toughness Round Robin Data – The "EURO" Fracture Toughness Curve*, VTT, Publications 367, VTT Technical Research Centre of Finland, Espoo 1998.